Biofilm 7 (2024) 100199

Contents lists available at ScienceDirect

Biofilm

journal homepage: www.sciencedirect.com/journal/biofilm

The effect of dental material type and masticatory forces on periodontitis-derived subgingival microbiomes

Carolina Montoya [a], Divyashri Baraniya [b], Tsute Chen [c], Nezar Noor Al-Hebshi [b,**], Santiago Orrego [a,d,*]

[a] Smart Biomaterials Laboratory, Department of Oral Health Sciences, Kornberg School of Dentistry, Temple University, Philadelphia, PA, USA
[b] Oral Microbiome Research Laboratory, Department of Oral Health Sciences, Kornberg School of Dentistry, Temple University, Philadelphia, PA, USA
[c] Department of Microbiology, Forsyth Institute, Cambridge, MA, USA
[d] Bioengineering Department, College of Engineering, Temple University, Philadelphia, PA, USA

ARTICLE INFO

Keywords:
Biomaterial-microbiome interactions
Oral microbiome
Periodontitis
Microbiota
Dysbiosis
Dental materials
Biomaterials
Biofilm
Oral infections
Piezoelectric
Barium titanate
Hydroxyapatite
Composites
Subgingival

ABSTRACT

Restorative dental materials can frequently extend below the gingival margin, serving as a potential haven for microbial colonization, and altering the local oral microbiome to ignite infection. However, the contribution of dental materials on driving changes of the composition of the subgingival microbiome is under-investigated. This study evaluated the microbiome-modulating properties of three biomaterials, namely resin dental composites (COM), antimicrobial piezoelectric composites (BTO), and hydroxyapatite (HA), using an optimized *in vitro* subgingival microbiome model derived from patients with periodontal disease. Dental materials were subjected to static or cyclic loading (mastication forces) during biofilm growth. Microbiome composition was assessed by 16S rRNA gene sequencing. Dysbiosis was measured in terms of subgingival microbial dysbiosis index (SMDI). Biomaterials subjected to cyclic masticatory loads were associated with enhanced biofilm viability except on the antibacterial composite. Biomaterials held static were associated with increased biofilm biomass, especially on HA surfaces. Overall, the microbiome richness (Chao index) was similar for all the biomaterials and loading conditions. However, the microbiome diversity (Shannon index) for the HA beams was significantly different than both composites. In addition, beta diversity analysis revealed significant differences between composites and HA biomaterials, and between both loading conditions (static and cyclic). Under static conditions, microbiomes formed over HA surfaces resulted in increased dysbiosis compared to composites through the enrichment of periopathogens, including *Porphyromonas gingivalis*, *Porphyromonas endodontalis*, and *Fretibacterium* spp., and depletion of commensals such as *Granulicatella* and *Streptococcus* spp. Interestingly, cyclic loading reversed the dysbiosis of microbiomes formed over HA (depletion of periopathogenes) but increased the dysbiosis of microbiomes formed over composites (enrichment of *Porphyromonas gingivalis* and *Fusobacterim nucleatum*). Comparison of species formed on both composites (control and antibacterial) showed some differences. Commercial composites enriched *Selenomonas* spp. and depleted *Campylobacter concisus*. Piezoelectric composites effectively controlled the microbiome viability without significantly impacting the species abundance. Findings of this work open new understandings of the effects of different biomaterials on the modulation of oral biofilms and the relationship with oral subgingival infections.

1. Introduction

Periodontitis is a common oral disease affecting half of the adults in the United States, and severe cases report a prevalence of 11% globally [1–3]. Periodontitis is induced by imbalanced (dysbiotic) microbial biofilm communities accumulating on the tooth surface below the gingival margin (subgingival plaque) [4,5]. Dysbiosis involves an increased biofilm biomass, a reduction in the proportion of symbiotic species, and an increase in the levels of pathobionts [6–10]. Enrichment of periodontal pathogens triggers an inflammatory response that initiates the gradual destruction of the periodontium tissues and bone, ultimately resulting in tooth loss [7,11]. Subgingival dysbiosis is majorly

* Corresponding author. 3223 North Broad Street, AEGD Clinic - Room 2E15, Philadelphia, PA, 19140, USA.
** Corresponding author.
E-mail addresses: alhebshi@temple.edu (N.N. Al-Hebshi), sorrego@temple.edu (S. Orrego).

https://doi.org/10.1016/j.bioflm.2024.100199
Received 9 March 2024; Received in revised form 19 April 2024; Accepted 4 May 2024
Available online 8 May 2024

driven by the host (i.e., genetics, age, systemic health) and different environmental factors (i.e., smoking condition, oral hygiene, certain medications) [12–15]. Disruption of periodontal microbiota may contribute to several chronic diseases such as endocarditis, osteoporosis, and rheumatoid arthritis [16–18]. A balanced and healthy periodontal microbiota is fundamental for balanced oral and systemic health.

Microbial organisms attach to living (biotic) and non-living (abiotic) biomaterial surfaces [19–21]. The interactions between oral microbes and biomaterials are controlled by different biomaterial surface properties, including wettability, chemistry, roughness, topography, stiffness, and potentially their combination [22,23]. For instance, increased biofilm quantity and virulence are positively correlated with an increase in the biomaterial surface roughness and hydrophobicity [23]. Dental biomaterials are commonly used for filling tooth cavities and for treating oral infections [24,25]. In the treatment of tooth sensitivity and discoloration, and carious and non-carious cervical lesions, biomaterials frequently extend below the gingival margin [26,27]. These subgingival restorations may result in an increased accumulation of plaque, gingival inflammation, periodontal destruction, increased pocket depth, loss of attachment, and gingival recession [28]. In fact, Class V restorations treated with composites have reported negative effects on the quantity and quality of subgingival plaque [29], affecting the subgingival microbial ecology and the susceptibility to the progression of periodontal diseases [29,30]. Thus, understanding how different biomaterials may drive changes in the subgingival microbiome is relevant for understanding the development of periodontal diseases.

Lab models of microcosm biofilms using subgingival plaque derived from periodontitis patients as inocula have successfully reproduced the intricate composition of in vivo periodontitis-associated subgingival microbiome [31–33]. However, these models have not been exploited to assess the effect of biomaterial type on microbiome composition neither the impact of the mastication forces applied over biomaterial surfaces where biofilms form. For example, Class V restorations are more susceptible to flexure forces during mastication compared to other restoration types [34]. We recently revealed that this biomechanical factor drives the pathogenesis of *Candida albicans* by increasing the virulence and biofilm quantity [35]. However, how such forces affect the periodontal microbiota is unknown. Mastication forces are integral for maintaining oral health and are the main factor affecting the behavior of the supporting periodontium, with dental biofilms challenging the integrity of these tissues [36–41]. Thus, understanding how repetitive forces applied over biomaterial surfaces affect microbe-biomaterials interactions, biofilm formation, and dysbiosis within a periodontal microenvironment is relevant.

Advanced biomaterials have been successfully used to treat periodontal disease by offering different therapeutic effects, including antimicrobial, immunomodulatory, and tissue regeneration effects [42,43]. To accomplish successful treatment, these biomaterials deliver different biophysical and bioactive cues that modify the microenvironment in the periodontium [44]. For example, antimicrobial biomaterials suppress pathogens by delivering different compounds, including antibiotics (e.g., minocycline), charged monomers (e.g., quaternary ammonium), and fillers (e.g., silver) [44–47]. In our recent works, we developed novel antimicrobial dental materials by harnessing the power of piezoelectric materials [48–50]. One study showed that piezoelectric charges elicit antimicrobial effects against a gram-negative fundamental periodontal pathogen (*Porphyromonas gingivalis*) [50]. The electrical charges prevented biofilm formation and reduced the number of viable cells. How piezoelectric materials modulate the entire subgingival microbiome under realistic subgingival conditions remains unclear. In this work, for the first time, we examined the effect of mastication forces applied to different dental biomaterials on the modulation of the periodontitis-derived subgingival microbiota. In addition, we examined for the first time whether piezoelectric charges continue to offer antibacterial effects against a diseased periodontal microbiota.

2. Materials and methods

The study was performed in accordance with the Declaration of Helsinki and approved by the school's Institutional Review Board (protocol #26456). Informed written consent was obtained from all subjects who donated saliva or subgingival plaque samples.

2.1. Fabrication of composites and verification of surface properties

Two resin composites were used for evaluating the microbiome modulation, including a commercial resin composite (control with no antibacterial effect; COM) and a piezoelectric resin composite (antibacterial effect). The piezoelectric composites (BTO) were fabricated by mixing a commercial dental resin (*3M* Filtek™ *Supreme Ultra Universal Restorative*) with 6.5 wt% of silanized nanoparticles of barium titanate (US Nanomaterials US3830, 200 nm). The quantity of the piezoelectric filler was selected based on an optimization method that included different properties such as mechanical properties, water sorption, solubility, degree of conversion, and electrical charge generation (see. **Supplemental Information-1** (SI-1)). Mixing of the resin and piezoelectric fillers was conducted using a planetary mixer (Thinky ARE-310) for 3 min at 2000 rpm. The COM group was prepared with the same resin composite (3M Filtek) without the piezoelectric fillers. To fabricate beams, the uncured composites were added into a metal mold with the desired shape ($1.6 \times 0.8 \times 13$ mm^3). A Mylar film was placed over the material surfaces to guarantee similar surface roughness along the sample surfaces. Composites were cured with a verified LED unit (Cure TC-3, Spring Health Products) for 1 min on each side, corresponding to a total radiant exposure of 166 J/cm^2. To align the electric dipoles and increase the electrical conversion in the piezoelectric composite, beams were subjected to a high electric field (20 kV/mm) at 140 °C for 40 min (poling). After curing, all composite samples were stored in distilled water for 24 h at 37 °C to release unreacted monomers that could interfere with microbiome growth [51].

HA beams (BioSurface Technologies Corporation) were selected as an additional biomaterial group due to its similarity to the mineral component of dental hard tissues (enamel, cement) present in the subgingival microenvironment due to the recession of the gingival margin in periodontal disease [52]. Before testing, a contact profilometer (Phase II SRG-4600) was used to verify the surface roughness of all samples ($Ra < 0.2$ μm) that could interfere with biofilm growth [53] (SI-2). The sessile drop method was used to measure the water contact angle of each group of samples (SI-3). Before experimentation, all beams were sterilized in a 70 % ethanol solution for 15 min, followed by air drying inside a biological safety cabinet under UV light (254 nm).

2.2. Biomaterial-microbiome biofilm model

2.2.1. Salivary pellicle coating

All beams were coated with a salivary pellicle layer to represent proteins found in the oral cavity that could mediate microbe adhesion [54]. Healthy young donors ($N = 40$) without systemic disease treatments, active caries lesions, or periodontal disease provided 5–10 mL of unstimulated saliva in sterile tubes. Volunteers were instructed to abstain from eating or drinking for at least 2 h before donation. After collection, all the individual saliva samples were pooled, centrifuged at 5000 rpm for 15 min, and treated with 2.5 mM dithiothreitol (PRV3151, Promega) for 10 min [54,55]. The resulting mixture was then combined with phosphate-buffered saline (PBS) in a 1:1 ratio, sterilized using a 0.2 μm membrane filter, and stored at −20 °C. Before inoculation and to form the saliva pellicle layer, beams were incubated for 16 h in 500 μL of pre-reduced sterile saliva at 37 °C under anaerobic conditions.

2.2.2. Clinical inocula

Subgingival dental plaque was used as inoculum in the model. Plaque samples were collected at the Periodontics Clinics of the Kornberg

School of Dentistry from 7 patients with moderate to severe periodontitis (SI-4), which was defined as having at least one tooth per quadrant with bleeding on probing, pocket depth ≥ 5 mm, and attachment loss ≥4 mm. An absorbent paper points (#40, Roydent) was inserted into the base of the periodontal pocket and gently moved around for 30 s for plaque collection. Four samples were collected per subject (the deepest pocket per quadrant), pooled into 1 mL of reduced transport fluid (RTF) [32,56], and immediately placed on ice and transported to the lab (collection time not more than 30 min). The samples from the 7 subjects were eventually mixed and used as an inoculum on the same day of collection (Fig. 1a). The selected number of donors have shown reproducible results regarding major bacterial species and similar composition patterns [57].

2.2.3. *Microbiome culture over biomaterials under cyclic loading and static conditions*

Sterile pooled human saliva supplemented with 2 % (v/v) heat-inactivated human serum (H3667 Sigma, USA) was used as the growth medium. This medium has been shown to grow periodontitis-derived microbiomes with the highest similarity to the clinical inocula [32,58]. Pellicle-coated beams were placed in the bottom of polystyrene wells, before adding 950 μL of the media and 50 μL of the inoculum to each well. To avoid media evaporation, 100 μL of mineral oil (M5904 sigma, USA) was added [59]. The biofilms were grown under anaerobic conditions (5 % H_2, 5 % CO_2, 90 % N_2) for 7 days at 37 °C. On day 3.5, the media was replenished. The three groups of materials (COM, BTO, HA) were subjected to two loading conditions: cyclic loading and static (no loading). The cyclic loading condition was designed to closely simulate the chewing forces applied over biomaterials/dental tissue during clinical service [27]. Beams were subjected to a 3-point bending configuration (span: 11 mm) using an actuator (MechanoCulture TX) applying $P_{min} = 0.5$ to $P_{max} = 2.0$ N at 2 Hz. The selected load magnitude resembles average stresses found in the clinical setting for Class V restorations (~22 MPa) [60]. The cyclic loading was set to activate 5 times/day for 15 min during the cell culture to simulate eating periods. This loading condition also activates the electrical charge generation (enables antimicrobial effect) of the piezoelectric composites group. After the incubation period, the tension side and borders of the beams were gently cleaned with a cell scraper. Only the biofilm formed on the compression side of the beam (region of interest) was used for evaluations. Beams were gently rinsed with PBS for removal of non-attached cells and evaluated for microbiome-biomaterial interactions. Two independent experiments (biological replicates) were carried out, each with a different clinical inoculum. Each experiment included 3 technical

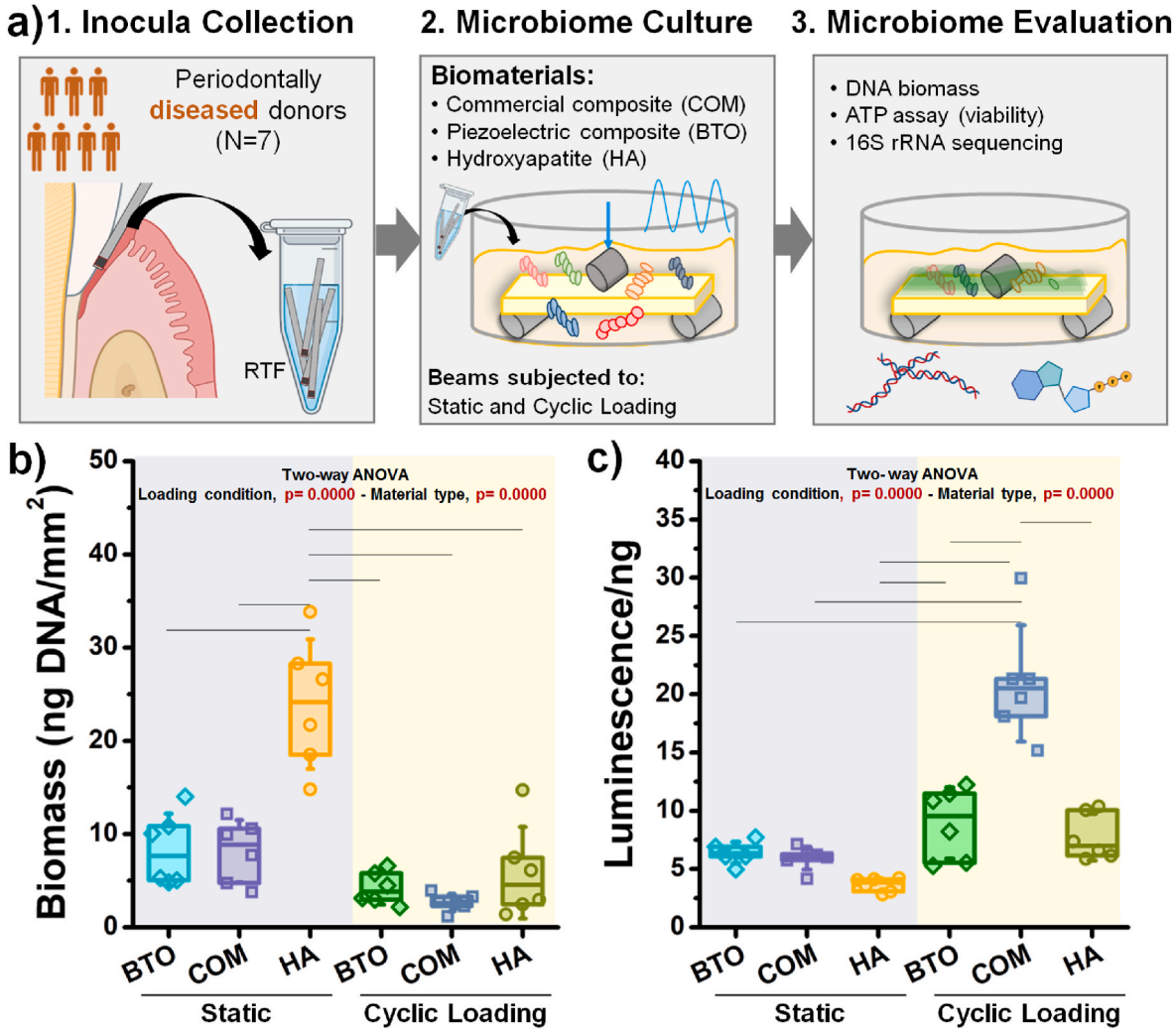

Fig. 1. Microbiome-biomaterial interactions. a) Flow chart of the experimental design and microbiome model. Periodontitis-derived microbiomes were grown for 7 days over three biomaterial types (commercial composites, piezoelectric composites, and hydroxyapatite) subjected to cyclic loading or static conditions. The generated microbiomes were evaluated for biomass and viability. b) DNA biomass of the microbiomes measured in terms of DNA yield. c) Viability of the microbiomes. The relative luminescence was normalized with the microbiome biomass. N = 6 samples for each evaluation. Lines above the boxes correspond to groups with statistical differences ($p < 0.05$). BTO: piezoelectric composite, COM: commercial composite, HA: hydroxyapatite beams.

replicates per group/condition. An aliquot of each inoculum was used for DNA extraction and sequencing in duplicates.

2.3. Evaluations of the biomaterial-microbiome interactions

2.3.1. DNA extraction and biomass assessment

DNA was extracted from the biofilms using the PureLink Microbiome DNA Purification kit (A29790, Invitrogen) following the manufacturer's instructions with a modification, namely that the beat beating and lysis steps were performed directly on the beams. Bead beating was done for 3 × 30 s cycles at 6 m/s (MP Biomedicals FastPrep). DNA yield and quality were assessed using a NanoDrop (Thermo Fisher Scientific). An estimate of the microbiome biomass was measured in terms of DNA yield in nano-grams (ng) and normalized by the surface area occupied by the biofilm on the beam (ng/mm^2). The DNA extracts were stored at −80 °C until sequencing.

2.3.2. ATP assay (viability assessment)

Viability of the microbiomes was assessed using an ATP assay (BacTiter-Glo assay, Promega, USA) according to the manufacturer's instructions. Briefly, beams were placed in an empty well, and PBS and BacTiter-Glo™ reagent (400 μL each) were carefully added. Samples were incubated in the dark at room temperature for 5 min with shaking before total luminescence was measured. Next, aliquots (200 μL) of the PBS/BacTiter-Glo™ solution were transferred to a white 96-well plate. The luminescence signal was recorded using a multi-mode microplate reader (Synergy HTX, Biotek, USA) and normalized by biomass.

2.3.3. 16S rRNA sequencing and bioinformatic analysis

Degenerate primers 27FYM [61] and 519R [62] with index sequences were used to amplify the V1–V3 region of the 16S rRNA gene. The resultant indexed amplicon libraries were sequenced on an Illumina Miseq platform using 2*300 bp chemistry at the Integrated Microbiome Resource (IMR, Halifax, Canada). Resultant paired-end reads were merged with PEAR [63] and pre-processed (trimming, quality filtration, and chimera check) with mothur [64] as previously described [65] (SI-5). The high-quality reads were then classified to the species level using our previously described BLASTn-based algorithm [65,66]. Taxon count tables, species richness and alpha diversity (Chao and Shannon Index) were computed using Quantitative Insights into Microbial Ecology (QIIME2) [67]. For assessing beta diversity, principal component analysis (PCA) was performed on centered log-ratio (CLR)-transformed species counts using microbiome [68] and phyloseq [69] packages in R. MaAsLin2 (Microbiome Multivariable Associations with Linear Models) package in R was applied to CLR-transformed counts to identify differentially abundant genera and species between test groups [70]. The Subgingival Microbial Dysbiosis Index (SMDI), as a summary statistic of the composition of the microbiomes was calculated for the individual samples as previously described [71].

2.3.4. Statistical analysis

All data is presented as box plots. Whiskers correspond to the standard deviation. The top of each box corresponds to the 25th percentile and the bottom to the 75th percentile. Statistical differences in the results (DNA biomass, ATP assay, alpha diversity, and the SMDI index) were evaluated using two-way analysis of variance (ANOVA) with loading condition and material type as variables, followed by Bonferroni pairwise comparisons. Adonis PERMANOVA (permutational analysis of variance) was used to estimate the differences in beta diversity with a significance of 0.05, adjusted for multiple comparisons. All the statistical analyses were performed in R.

3. Results

3.1. Cyclic loading applied to biomaterials reduces microbiome biomass but enhances viability

The microbial DNA biomass and viability of the microbiomes formed over the different biomaterials subjected to cyclic loading or held static were assessed (Fig. 1bc). Overall, significant differences in the microbiome's biomass in terms of the biomaterial type and loading condition ($p < 0.05$) were observed (Fig. 1b). The highest biomass was noted in microbiomes formed over the HA surfaces held under static conditions. Applying cyclic loading to the biomaterials significantly reduced the microbiome biomass for all biomaterials. Similar quantities of biomass were observed for the three biomaterials (COM, BTO, HA) under cyclic loading. The microbiome viability depended on the biomaterial type and loading condition ($p < 0.05$) (Fig. 1c). The highest viability was observed for microbiomes grown over the COM beams under cyclic loading conditions, whereas the lowest was observed for those under static conditions regardless of the biomaterial type. Overall, the application of cyclic loading resulted in a significant increase in the viability of the microbiomes. Focusing on the antibacterial composite (BTO), the viability was similar and independent of the loading conditions (static versus cyclic). The lower viability observed in the cyclic loading indicates the action of the antibacterial effects caused by the electric charges.

3.2. Microbiome profiles of periodontitis-derived biofilms compared to clinical inocula

The clinical inocula rendered an average of 176 species, distributed in 9 phyla, 52 genera. In the *in vitro* grown microbiomes, the number of observed species differed by biomaterial type and loading conditions being lowest on HA under loading conditions (73 species) and highest on HA under static conditions (121 species). On average, 96 species were observed in the microbiomes formed over the composite materials (BTO and COM) and independent of the loading condition. The clinical inocula showed a closely even distribution of Firmicutes (27 %), Fusobacteria (26 %), and Bacteroidetes (31 %) (Fig. 2a). The remaining phyla were Proteobacteria (4 %), Spirochaetes (5.6 %) and Synergistetes (3.5 %). A major shift in this relative species abundance of the microbiomes formed over the biomaterials, particularly those grown on HA, was observed. Under static loading, microbiomes on HA beams were dominated by Bacteroidetes (65 %) at the expense of Firmicutes (20 %) and Fusobacteria (12 %), while under cyclic loading, they showed an increase in Firmicutes (91 %) at the expense of Fusobacteria, and Bacteroidetes (<7 %). On average, the microbiomes grown on composites were dominated by Firmicutes (40–60 %), followed by Bacteroidetes (23–37 %), and Fusobacteria (11–25 %). Phylum distributions were less skewed in the microbiomes formed over composites (BTO and COM), especially under cyclic loading conditions.

At the genus level, the dominant genera in the clinical inocula were *Fusobacterium* (24 %), *Porphyromonas* (14 %), *Prevotella* (9 %), and *Streptococcus* (8 %) (Fig. 2b). HA beams held static enriched *Porphyromonas* (58 %), while the application of cyclic loading resulted in the overgrowth of *Streptococcus* (27 %) at the expense of *Porphyromonas*. Inversely, both composites enriched *Streptococcus* under static conditions including COM from 11 % to 21 % and BTO from 7 % to 20 %. In addition, both composites enriched *Porphyromonas* under cyclic conditions including COM from 5 % to 24 % and BTO from 13 % to 19 %. *Parvimonas* was over-represented on all biomaterial types (3–10 %).

At the species level, the average microbiome in the clinical inocula was dominated by *Fusobacterium nucleatum* (21 % for the subspecies combined), *P. gingivalis* (9 %), *Porphyromonas endodontalis* (5 %), *Prevotella intermedia* (3 %) and *Filifactor alocis* (3 %), together making ~40 % of the microbiome (Fig. 2c). In comparison, HA beams held static showed an overgrowth of *P. gingivalis* (52 %) and *Parvimonas micra* (6

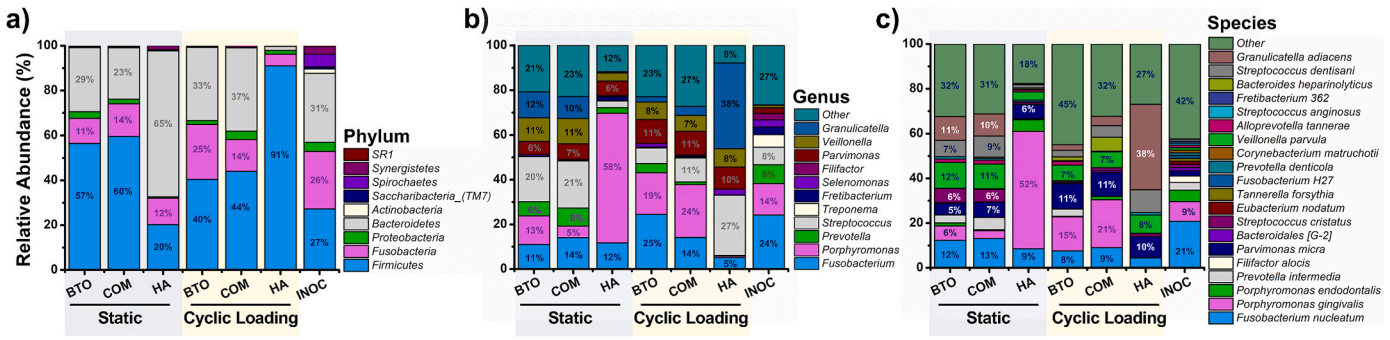

Fig. 2. Microbial profiles of periodontitis-derived microbiomes by biomaterial type and loading condition, compared to the clinical inocula. Relative abundances at the a) phylum, b) genus, and c) species levels. Taxa are ordered by abundance with respect to the clinical inocula. BTO: piezoelectric composite, COM: commercial composite, HA: hydroxyapatite beams, INOC: clinical inocula.

%), at the expense of *F. nucleatum* (9 %); together the three species accounted for 67 % of the average microbiome. Under cyclic loading, HA resulted in sharp increase in the abundance of *Granulicatella adiacens* (38 %), followed by *Streptococcus dentisani* (10 %), and *P. micra* (10 %), accounting for 58 % of the average microbiome. The most abundant species in the microbiomes grown on both composites (COM and BTO) under static conditions were *F. nucleatum* (13 %), *Veillonella parvula group* (11 %), *G. adiacens* (10 %), *S. dentisani (8 %)*, *P. micra* (6 %), *Streptococcus cristatus* (6 %) and *P. gingivalis* (5 %), accounting for 59 % of the microbiome. However, under cycling loading, BTO and COM composites were dominated by *P. gingivalis* (18 %), *P. micra* (11 %), *V. parvula group* (7 %), unclassified *Fusobacterium* species (5 %) and *Fusobacterium oral taxon 370* (5 %). Overall, the microbiome profiles were similar for the two biological replicates demonstrating the reproducibility of the results (see. SI-6).

3.3. Biomaterial type and cyclic loading affects alpha diversity (richness/evenness)

The microbiome alpha diversity was estimated using the Chao (expected richness) and Shannon (richness and evenness) indexes. Both indices were highest in the clinical inocula. Neither biomaterial type ($p = 0.9202$) nor loading conditions ($p = 0.1080$) influenced the number of species found in the microbiome (Fig. 3a). Similarly, no significant differences were observed in the Shannon index associated with the application of cyclic loading ($p = 0.1241$) (Fig. 3b). However, the biomaterial type significantly affected Shannon index ($p = 0.0001$). Namely, HA beams subjected to cyclic loading rendered the lowest Shannon index of the microbiome. This suggests that the biomaterial surface properties (e.g., chemistry, stiffness) and loading condition of HA is favoring the overgrowth of certain species (Bacteroides and Firmicutes - see Fig. 2) compared to composites. Similar richness and evenness (Shannon index) of microbiomes formed over both composites were observed. This observation suggests that the electrical charges applied by the BTO group (i.e., activation of the antibacterial effect) is not depleting the number of microbes, nor disturbing the potential balance of the microbiome as the broad-spectrum antibiotics does.

3.4. Effect of biomaterial type on beta diversity and specific bacterial species

Microbiome compositional variations (beta diversity) were determined via PCA analysis for the tested biomaterials ranked by loading condition as presented in Fig. 4a and b. Overall, the microbiome composition of the clinical inocula and those formed over the biomaterial beams (regardless of loading conditions) were significantly different, forming two separate main clusters. The composition of the microbiomes grown on HA was significantly different from those grown

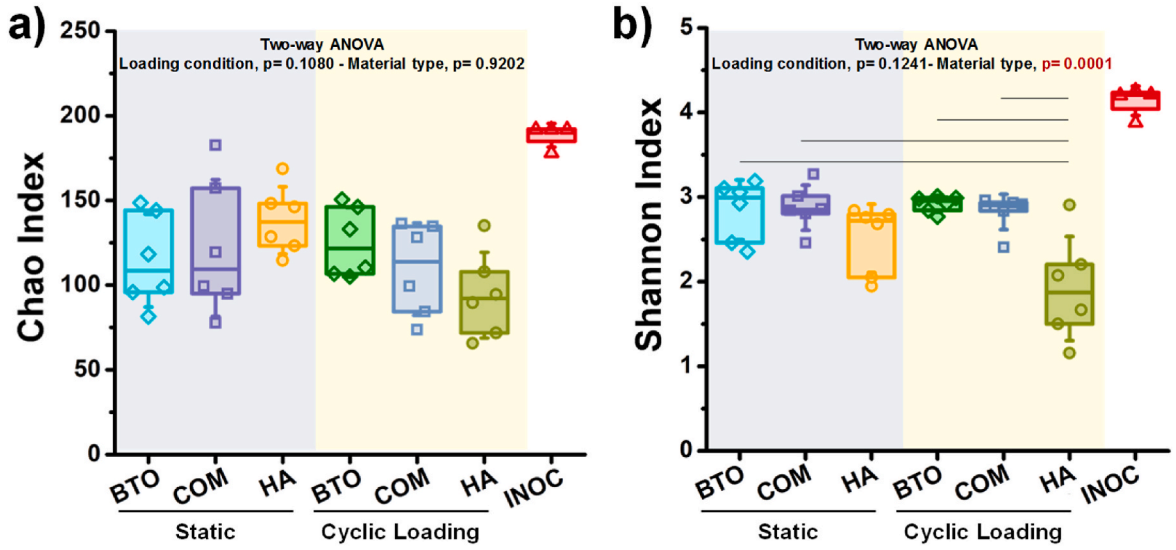

Fig. 3. The expected richness and evenness of the periodontitis-derived microbiomes by biomaterial type and loading condition. Alpha diversity metrics included a) Chao and b) Shannon index. Lines above the boxes correspond to groups with statistical differences ($p < 0.05$). BTO: piezoelectric composite, COM: commercial composite, HA: hydroxyapatite beams. INOC: clinical inocula.

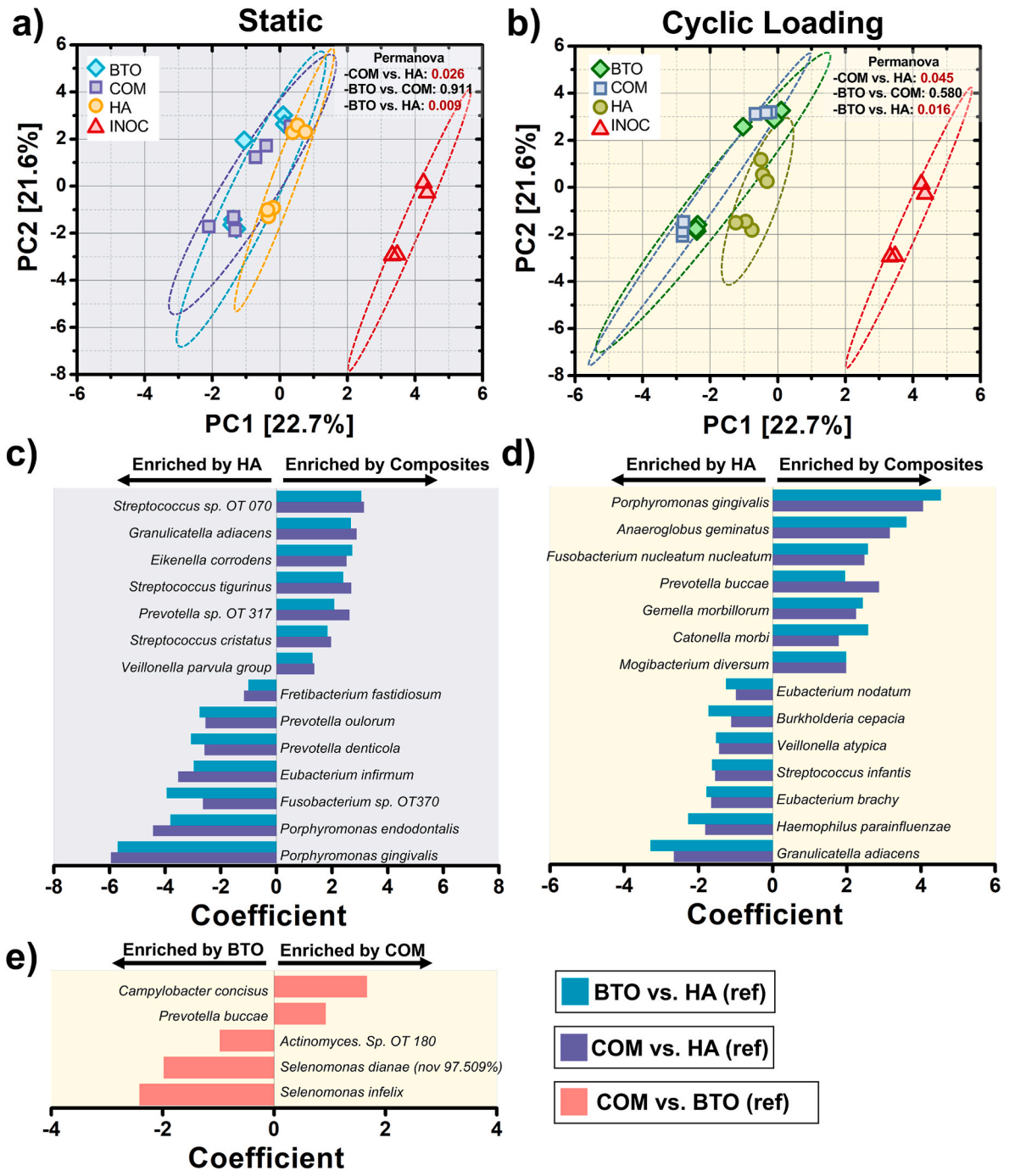

Fig. 4. Principal component analysis (PCA) plots of periodontitis-derived microbiomes cultured over biomaterials subjected to a) static and b) cyclic loading conditions. Differences in the microbiome compositions were assessed with PERMANOVA ($p \leq 0.05$). Centered log ratio (CLR) transformed data were analyzed with Multivariate Association with Linear Models (MaAsLin2) to identify differentially abundant taxa in the microbiomes grown on hydroxyapatite compared to those grown on both piezoelectric and commercial composites under c) static and d) cyclic loading conditions. e) Differentially abundant species between microbiomes grown on commercial composites and piezoelectric composites under cyclic loading conditions. Differences with FDR ≤0.05 and −1.5>coefficient>1.5 were considered significant. BTO: piezoelectric composite, COM: commercial composite, HA: hydroxyapatite beams, INOC: clinical inocula.

on either composite type (BTO and COM) subjected to both static ($p = 0.026$ for PERMANOVA in COM vs. HA; $p = 0.009$ for PERMANOVA in BTO vs. HA) and cyclic loading conditions ($p = 0.045$ for PERMANOVA in COM vs. HA; $p = 0.016$ for PERMANOVA in BTO vs. HA). No significant differences in beta diversity were observed for the microbiomes grown over both composites including BTO (Fig. 5a) ($p = 0.140$, PERMANOVA) and COM (Fig. 5b) ($p = 0.088$, PERMANOVA). No differences in beta diversity were observed between BTO and COM composites regardless of loading condition. Overall, these results suggest that the biomaterial surface properties (composites versus hydroxyapatite) rendered microbiomes with different microbial compositions.

Differential abundance analysis was conducted to identify statistically significant differences (FDR ≤0.05) in the abundances of species as a function of biomaterial type stratified by loading conditions (Fig. 4c and d). Under static conditions, both composite biomaterials similarly enriched predominantly health-associated species, including *Streptococcus* spp., *G. adiacens*, and *V. parvula* compared to HA, while the latter mostly enriched periodontal pathogens, including *P. gingivalis, P.*

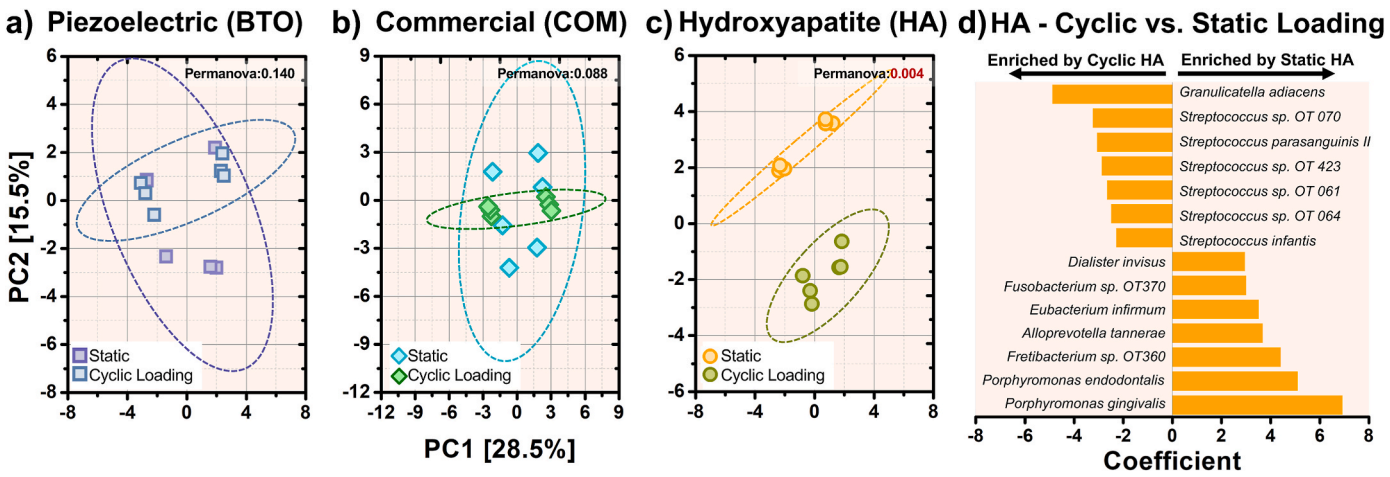

Fig. 5. Principal component analysis (PCA) plots of periodontitis-derived microbiomes cultured on a) piezoelectric composites, b) commercial composites, and c) hydroxyapatite beams subjected to static or cyclic loading conditions. Differences in the microbiome compositions were assessed with PERMANOVA ($p \leq 0.05$). d) Differentially abundant species between microbiomes grown on hydroxyapatite beams under static and loading conditions. Differences with FDR ≤0.05 and −1.5>coefficient>1.5 were considered significant. BTO: piezoelectric composite, COM: commercial composite, HA: hydroxyapatite beams.

endodontalis, Eubacterium infirmum, and *Fretibacterium fastidiosum* (Fig. 4c). Under cyclic loading, COM and BTO composites enriched a mixture of pathobionts (*P. gingivalis* and *Anaeroglobus geminatus)* and health-associated species *(Gemella morbillorum)* and core species (*F. nucleatum, and Catonella morbi*) compared to HA (Fig. 4d). HA beams enriched a different set of pathobionts (*Eubacterium brachy* and *Eubacterium nodatum)* and health-associated species including *G. adiacens*, *Haemophilus parainfluenzae, Streptococcus infantis,* and *Veillonella atypica*. Overall, these results suggest that cyclic loading of HA beams promoted a shift towards health-associated species, whereas both composites had an inverse effect. To reveal the potential antimicrobial effect of piezoelectric charges, an additional comparison was performed between COM and BTO subjected to cyclic loading (Fig. 4e). Commercial beams resulted in a significant enrichment of *Campylobacter concisus* and *Prevotella buccae*. Piezoelectric charges targeted the depletion of *Selenomonas infelix*, *Selenomonas dianae*, *Actinomyces Sp. OT 180* (Fig. 4e). No significant differences between BTO and COM were observed under static conditions.

3.5. Effect of the loading condition on beta diversity and specific bacterial species

Microbiome compositional variations (beta diversity) associated with the loading condition (cyclic loading versus static) for each biomaterial type are presented in Fig. 5a–c. No differences in beta diversity were observed for the microbiomes grown over both composites, namely BTO (Fig. 5a) ($p = 0.140$, PERMANOVA) and COM (Fig. 5b) ($p =$ 0.088, PERMANOVA). The case was different for HA beams. Microbiomes grown in HA under static and loading conditions were significantly different ($p = 0.004$, PERMANOVA) (Fig. 5c). This suggests that the combination of biomaterial surface properties and cyclic loading changes microbiome diversity. To identify these changes driven by cyclic loading, differential abundance analysis was conducted (Fig. 5d). HA under static condition enriched predominantly periodontal pathogens, including *P. gingivalis, P. endodontalis,* and *E. infirmum.* Cyclic loading of the HA beams resulted in the depletion of *P. gingivalis* and the enrichment of predominantly health-associated species including *Streptococcus* spp. and *G. adiacens.* The relative abundances of selected differentially abundant species is presented in SI-7.

3.6. Effect of biomaterial type and loading on subgingival dysbiosis

The overall effect of biomaterial and loading condition on driving dysbiosis was measured using the SMDI parameter (Fig. 6). Higher SMDI (>0) indicates dysbiotic periodontal microbiomes, whereas lower values (<0) correspond to a normobiotic behavior [71]. The highest SMDI was calculated for the clinical inocula (SMDI = 3.7), confirming the degree of disease of collected plaque. The application of cyclic loading and the biomaterial type significantly affected the SMDI ($p < 0.05$). However, looking into the biomaterials subjected to static loading, higher SMDI was determined for HA samples (SMDI = 1.3) compared to the composite materials (SMDI = 0.16). All biomaterials under cyclic loading showed a similar index (SMDI~0.24).

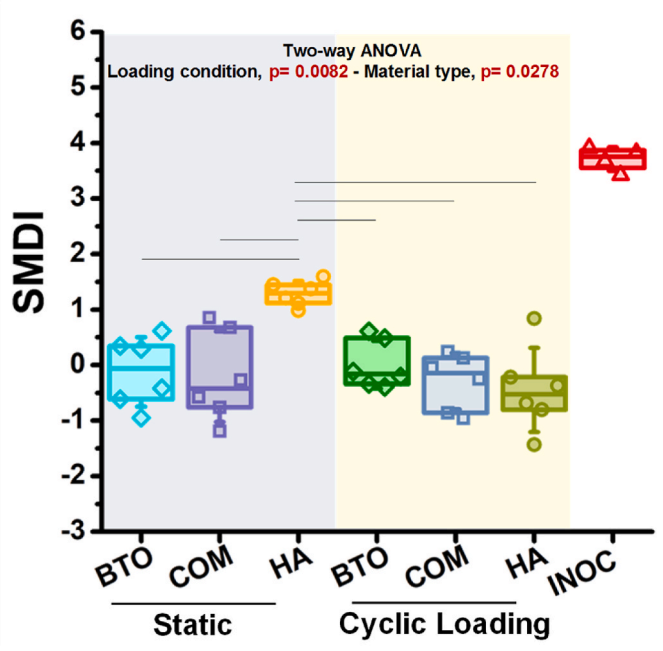

Fig. 6. Subgingival microbial dysbiosis index (SMDI) of periodontitis-derived microbiomes obtained by biomaterial type, loading condition and clinical inocula calculated as previously described [71]. Higher SMDI (>0) indicates dysbiotic periodontal microbiomes, whereas lower values (<0) correspond to normobiotic behavior. Lines above the boxes correspond to groups with statistical differences ($p < 0.05$). BTO: piezoelectric composite, COM: commercial composite, HA: hydroxyapatite beams, INOC: clinical inocula.

4. Discussion

Periodontal dysbiosis results from a change in the microbiome composition which drives the destruction of the host tissues through enzymes and inflammatory mediators [72,73]. Changes in the microbiome composition can be attributed to multiple factors, including oral hygiene, diet, smoking, gingival inflammation, genetic background, and salivary flow [74–76]. Dental biomaterials have been traditionally used in the periodontium for therapeutic purposes (antimicrobial and tissue regeneration), in restorative practices, and for the modulation of the immune system [43,77]. The potential role of dental biomaterials in modulating the microbiome or fueling periodontitis is limited. In this study, for the first time, we evaluated the changes of periodontitis-derived subgingival microbiomes controlled by the interactions with three dental materials (resin composites, antibacterial piezoelectric composite, and enamel-like HA) subjected to repetitive mastication forces. Three major findings are reported in this study: First, both the physico-chemical properties of biomaterials and the application of cyclic loading are driving changes in the composition, abundance, and diversity of periodontal microbiome. Marked differences between microbiomes grown in composites and HA were observed. Cyclic loading applied to HA beams had a superior effect in modulating the microbiome than that of both composites. Second, HA surfaces held static favored the enrichment of known periodontal pathogens such as *P. gingivalis*, but the application of cyclic loading reversed it. Third, the effect of electrical charges from piezoelectric materials is significant in controlling the microbiome viability and poor in driving changes of the microbiome (diversity and species abundance) when compared to the commercial resin. However, a bacterial specie previously identified in triggering the host immune response during periodontal disease (*C. concisus*) was significantly depleted by piezoelectric composites [78].

Biomaterial properties driving changes of the microbiome: The interactions between dental biomaterials and microbes are known to be controlled by different biomaterial surface properties, including wettability, chemistry, roughness, topography, stiffness, and cyclic loading [22,23]. These studies are usually conducted using monoculture (single-specie) models that enable the detailed study of the adhesion and biofilm formation processes [78]. However, clinically, biofilms are composed of hundreds of species which can underpredict lab model outcomes. Our results showed striking differences in the microbiome formed over composites and enamel-like biomaterials. Compared to composites, static HA substrates supported the formation of microbiomes with the highest microbial biomass, lowest viability, and a significant increase in the abundance of *P. gingivalis*. To explain these differences, we looked at the physico-chemical properties of biomaterials. HA surfaces are hydrophilic (WCA = 32°) (SI-3) with a negative surface charge (−35 mV) [79,80], an average micro-roughness of Ra~0.16 μm (SI-2), an uneven topography (S_{dr} = 58 %) [81] and a stiffness of E = 80 GPa [82]. Compared to HA, composite surfaces are less hydrophilic (WCA = 52°) (SI-3), with a similar negative surface charge (−30 mV) [81], less rough (Ra~0.08 μm) (SI-2), more even topography (S_{dr} = 3 %) [81] and less stiff (E = 9 GPa) [83]. Generally, bacterial adhesion and biofilm formation is increased in biomaterial surfaces with higher roughness, hydrophilic, positively charged, uneven textures, less stiff (softer), and potentially interplay of those [23]. However, exploring different combinations of surface properties can provide deeper insights, given the intrinsic interdependence of surface parameters [23]. Recent studies showed highest *P. gingivalis* biofilm formation over rougher and more hydrophilic surfaces regardless of the biomaterial chemistry (zirconia or titanium alloys) [84]. Similarly, in another study using a saliva-derived microcosm model, the microbiome showed an increased abundance of *P. gingivalis* in biofilms formed over HA surfaces compared to stainless steel surfaces [85]. Rougher surfaces with lower contact angle (more hydrophilic) were measured for HA compared to stainless-steel. Our results agree with these studies, suggesting that rougher surfaces (more than contact angle and chemistry) favor the abundance of *P. gingivalis* in biofilms formed over HA surfaces. Nonetheless, conducting a systematic study controlling all the surface parameters (stiffness, topography) will provide an improved insight.

In the current study, the presence of high microbial biomass (Fig. 1b) and low viability (Fig. 1c) in static HA compared with other materials in static conditions can be explained by considering various factors specific to oral biofilm dynamics. The extracellular polymeric substances (EPS) of biofilms serve as a protective shield that encapsulates the bacteria complex, protecting them against attacks [86,87]. Up to 90 % of the total mass of biofilms is comprised of EPS, which may include bound water and various polymers like extracellular DNA (eDNA), polysaccharides, proteins, and lipids [88]. In addition, *P. gingivalis* produces a capsular polysaccharide, which encases the cell surface, contributing to the bacterial protection, aggregation, virulence, and modulation of the host inflammatory response [86,88]. The properties of EPS are impacted by different factors, including nutrition, salivary flow and shear rates, hydration, and the bacteria complex within the biofilm [89]. Specifically, Ca^{2+} ions play a role in consolidating biofilm structures in various bacterial species, including gram-negative [90–92]. This regulation may activate the transcription of genes responsible for producing surface adhesins and EPS [93]. Recent work showed that calcium ions are essential for growing *P. gingivalis*, but there is no evidence of the effect on EPS production. In our study, the surface roughness of HA surfaces after incubation was significantly increased (SI-2), suggesting a release of Ca^{2+} from the biomaterial surface. We hypothesize that these calcium ions are being uptake by the *P. gingivalis* cells to stimulate increased EPS production. An increase in EPS creates a more protective, dense matrix around the microbial cells, limiting the diffusion of nutrients and oxygen into the deeper layers of the biofilm. As a result, cells experience reduced metabolic activity [94,95]. However, future studies are required to measure this effect and specific changes in the *P. gingivalis* cells, such as the upregulation of bacterial surface proteins such as fimbriae and gingipain hemagglutinin. Finally, these results suggest that HA surfaces may offer a more "beneficial" environment in terms of reduced adherence of pathogenic species compared to composite materials, particularly under static conditions. The smoother and less hydrophilic nature of HA surfaces potentially limits the formation of biofilms enriched with pathogenic bacteria like *P. gingivalis*, indicating its potential as a favorable substrate for maintaining oral health.

Cyclic loading of biomaterials driving changes in the microbiome: The periodontium is a structure that serves as a shock absorber and tooth stabilization from masticatory/orthodontic forces [96]. Class-V restorations are challenged by repetitive mechanical stresses, which are partly responsible for low marginal adaptation, increased microleakage, and early failure of restorations [97,98]. When biomaterials experience cyclic loading, the surface repeatedly elongates back and forth. Over these "moving surfaces" is where microbes are adhering and forming biofilms. The magnitude of this "cyclic elongation" for both biomaterials is different. Composites and HA beams are experiencing an average displacement of 10 μm and 0.01 μm, respectively. In perspective, microorganisms in the oral microbiome vary widely in size, typically ranging from a few micrometers to sub-micrometer scales, with bacteria generally falling within the range of 0.5–5 μm. Microbes could be interpreting the cyclic elongation of the biomaterial surface as an external stressor or perturbation which can be driving changes in the microbiome. In fact, *C. albicans* triggered its virulence by this phenomenon [35], and in this study we are observing similar effects for the first time. As shown in Fig. 1b and c, applying cyclic loading decreased the microbiome biomass and increased the viability of the COM and HA microbiomes. In the oral cavity, dental plaques are stimulated with salivary and gingival crevicular fluid flow which influence bacterial adhesion and biofilm formation [23]. A study with periodontal biofilms subjected to dynamic fluid shear stress reported less biomass and loose structures than those without external flow [99]. It was suggested that fluid eddies can disrupt the adhesion bonds between biofilms and biomaterial surfaces [100]. Another study

using dental microcosm biofilms also found the effect of hydrodynamic shear on microbiome composition and architecture [101]. Microbial growth in the presence of hydrodynamic shear has been related to increased EPS production, irregular biofilm architecture, and reduced strength [102]. Although cyclic loading and hydrodynamic shear are two different forms of external stimuli affecting the behavior of biofilms, it indicates that these external stressors influence bacterial processes such as biofilm formation, gene expression, cell division, morphology, motility, and antibiotic resistance [103]. We hypothesize that similar to shear stress, the cyclic loading of biomaterials affects biofilm architecture and community composition by altering the composition of microbes adhered to the biomaterial surfaces. For example, under shear conditions, hydrophilic *Streptococcus* is easier to detach than more hydrophobic species such as *Actinomycetes* [104]. However, when the shear stress exceeds a threshold bacterial adhesion is inhibited [105]. Additional research is needed to understand this phenomenon.

Overall, cyclic loading of both biomaterials (composites and HA) had an inverse effect in microbiome composition. Specifically, cyclic loading in HA resulted in the complete depletion of *P. gingivalis* and *P. endodontalis* (Fig. 2c), which correlate directly with the decrease in the SMDI (Fig. 6). However, in loaded composites, *P. gingivalis* was enriched compared to static cases (Fig. 2c). Applying cyclic loading to biomaterials causes the surface where cells adhere and form biofilm to undergo repeated elongation and shortening. Early colonizers may be sensing the changes of the biomaterial surface which could be affecting their adhesion process. As a late colonizer, *P. gingivalis* attaches to early colonizing bacteria and participates in developing the biofilm structure [106]. In addition, high interactions between *F. nucleatum* and *P. gingivalis* have been observed [107]. It appears that the cyclic loading of HA surfaces is affecting the adhesion of early colonizers such as *Actinomyces* and *Streptococcus* and, in return, the interaction with *P. gingivalis* towards a complete depletion. It is known that *P. gingivalis* is a late colonizer since it prefers to co-aggregate with receptors from other oral bacteria (initial and secondary colonizers) than from receptors found in the salivary pellicle or biomaterial surface [108]. On the contrary, HA surfaces under cyclic loading seem to favor *G. adiacens and Streptococcus growth* (Fig. 5d). *G. adiacens*, a nutritional variant of the streptococcus species, is typically a health-associated species commonly found on mucosal surfaces. This specie is known to aggregate with *F. nucleatum*, which offers *Granulicatella* additional benefits for overgrowth [109]. In addition, *Streptococcus* species (which accounts for 27 % of the cyclically loaded HA microbiome) support the growth of *G. adiacens* by pyridoxal or L-cysteine [110]. Further studies are required to reveal the specific characteristics involved in the favor/disfavor of the cyclic loading of biomaterials on the enrichment/depletion of specific bacterial species. Evaluation of specific bacterial functional groups, membrane, and cell wall composition must be considered.

Piezoelectric charges driving changes in the microbiome: Piezoelectric composites subjected to cyclic loading produce electrical charges at the biomaterial surface where biofilms form. Electrical charges have been shown to control and reduce cell viability in bacteria through mechanisms such as membrane disruption, interference with cellular processes (e.g., ion imbalance), and induction of oxidative stress, ultimately leading to cell damage or death [44,111,112]. Results from this work are aligned with these findings. The magnitude of the electrical charges produced by the BTO (~1.2 pC/cm^2) were able to control the viability of the microbiome without significantly affecting the diversity/abundance of composites that could drive dysbiosis (Figs. 3b and 6). In addition, results from this work showed that cyclic loading of non-piezoelectric biomaterials (COM and HA) drives changes of the microbiome viability, diversity and abundance (Figs. 1b and 5). In other words, electrical charges are controlling the number of live cells without affecting the "balance" or type of species present in the microbiome formed over composites. The application of cyclic loading to other biomaterials (HA and COM) resulted in increased microbiome viability (static vs. cyclic) (Fig. 1c).

Overall, the electrical charges generated by the BTO composite decrease the viability of the microbiome without completely eliminating all the microbes or causing further imbalance in the periodontal microbiome as observed in Fig. 6. When compared to other biomaterials and loading conditions, BTO and COM exhibited notably lower levels of dysbiosis (as measured by the SMDI index) under static conditions, in contrast to HA beams. Furthermore, when subjected to cyclic loading conditions, all biomaterials demonstrated similar levels of dysbiosis. This could be attributed to the short and low electrical charge applied in this work (75 min/day). Our previous studies showed that when activated for 24 h in a single-species biofilm, 1.2 pC/cm^2 of charge generation were able to suppress the growth of *Streptococcus mutans* biofilms significantly (3log) [48]. In this study, BTO- producing electrical charges (cyclic) were not able to deplete the amount of *P. gingivalis*. However, our recent study using a piezoelectric hydrogel against *P. gingivalis* (single-species model) showed a 2–3 log reduction of this pathogen with 1 pC/cm^2 of charge generation [50]. Similar studies evaluating the antimicrobial effect of carolacton (antimicrobial agent) showed powerful effects in singles-species model, but poor performance in microcosm models [113,114]. The higher complexity and diversity, synergistic resistance, heterogeneity in metabolism, and adaptive responses of a multispecies microbiome appears to be challenging the efficacy of antibacterial dental materials [115]. In this study, only one electrical charge magnitude was tested. Future studies should consider a systematic study to evaluate how different electrical charges (>1.2 pC) affect the microbiome viability, bacterial composition, and dysbiosis. The application of piezoelectric charges to the periodontal microbiome could have implications in the inflammatory response during gingivitis or periodontal disease [115]. *Campylobacter concisus* promotes strong immunostimulatory activity through Toll-like receptor 4 (TLR4) stimulation [78]. BTO under cyclic loading significantly depleted the amount of *C. concisus* compared to COM. Depletion of *C. concisus* might reduce the activation of TLR4-mediated inflammatory pathways, potentially leading to a decrease in inflammatory response during the progression and development of periodontal disease.

Despite the potential impact of our findings, this study has limitations. First, our experiments used a saliva pellicle on the biomaterial's surfaces, which is required for bacterial adhesion. However, the presence of specific salivary proteins and their concentration are affected by different sterilization processes [116]. Second, to evaluate the mastication effect on the microbiome's modulation, only one magnitude of mechanical stress was assessed (22 MPa). Due to differences in the stiffness, the mechanical strain (deformation) on the biomaterial surface varied for each biomaterial. Future studies should evaluate how the magnitude of the different cyclic deformation affects the microbiome's species richness/diversity. Third, our study evaluated microbiomes cultivated only at one-time point (7 days). Evaluation of the microbiomes at incubation earlier times will add valuable information about the composition of early colonizers (i.e., *Streptococcus, Actinomyces,* and *Veillonella*) and their interaction with bridge organisms such as *Fusobacterium, Prevotella,* and *Capnocytophaga.* Prolonged incubation will affect the microbial composition within the microbiome. Some species may dominate, while others might decrease in abundance due to competition or changes in environmental conditions. Overall, the microbiomes generated on the biomaterials differed significantly from the clinical inocula, showing a significant drop in microbial diversity and dysbiosis (3.7 vs. 0.03). Such changes in alpha diversity were also observed in other *in vitro* models inoculated with healthy and cariogenic saliva [117–119]. Part of this change is likely associated with the *in vitro* culture model conditions (i.e., incubation time, nutrient availability, pH, etc.) [120]. *In vitro* conditions usually result in the loss of redundant species or species depending on specific host secretions [121]. There is an urgent need to optimize microcosm *in vitro* models to evaluate the interactions between oral microbes and biomaterials that enable a closer representation of clinical conditions and the comparison of all studies. Finally, our study obtained the clinical inocula from patients with

moderate to severe periodontitis to represent all clinically relevant species. However, future studies should include clinical inocula of patients at different periodontitis levels. Due to dissimilar ecological parameters such as oxygen tension and nutrient availability subgingival microbiomes could vary according to the disease stage [122].

In conclusion, this study evaluated the interactions between periodontitis-derived subgingival microbiomes and three different dental materials subjected to repetitive mastication patterns. Compared to resin composites, biofilms formed over hydroxyapatite substrate resulted in significant changes in microbiome composition and abundance but with similar diversity. Subjecting biomaterials to repetitive mechanical loading resulted in major microbiome changes for hydroxyapatite. The *Porphyromonas* genera was significantly abundant in the static hydroxyapatite but depleted in cyclic loading. Applying cyclic loading composites decreased the microbiome biomass but increased viability with similar composition, diversity, and evenness. Piezoelectric composites effectively controlled the microbiome biomass and viability without significantly impacting the species abundance and diversity. Results from this work advance the understanding of new bioactive dental materials that can modulate the oral microbiome.

CRediT authorship contribution statement

Carolina Montoya: Writing – review & editing, Writing – original draft, Visualization, Validation, Resources, Methodology, Investigation, Formal analysis, Data curation, Conceptualization. **Divyashri Baraniya:** Validation, Methodology, Formal analysis, Data curation. **Tsute Chen:** Validation, Methodology, Investigation, Formal analysis. **Nezar Noor Al-Hebshi:** Writing – review & editing, Validation, Supervision, Methodology, Investigation, Data curation, Conceptualization. **Santiago Orrego:** Writing – review & editing, Writing – original draft, Visualization, Validation, Supervision, Resources, Project administration, Methodology, Investigation, Funding acquisition, Formal analysis, Data curation, Conceptualization.

Declaration of competing interest

The authors declare that they have no known competing financial interests or personal relationships that could have appeared to influence the work reported in this paper.

Data availability

Data will be made available on request.

Acknowledgements

This work was supported by the National Institute of Dental and Craniofacial Research (NIDCR) Award R21-DE030564. This work was also supported in part by the Temple University Maurice Kornberg School of Dentistry start-up fund and by the Office of Provost at Temple University strategic fund.

Appendix A. Supplementary data

Supplementary data to this article can be found online at https://doi.org/10.1016/j.bioflm.2024.100199.

References

[1] Eke PI, Borgnakke WS, Genco RJ. Recent epidemiologic trends in periodontitis in the USA. Periodontology 2020;82(1):257–67. 2000.
[2] Eke PI, Thornton-Evans GO, Wei L, Borgnakke WS, Dye BA, Genco RJ. Periodontitis in US adults: national health and nutrition examination survey 2009-2014. J Am Dent Assoc 2018;149(7):576–88.
[3] Nazir M, Al-Ansari A, Al-Khalifa K, Alhareky M, Gaffar B, Almas K. Global prevalence of periodontal disease and lack of its surveillance. Sci World J 2020; 2020.
[4] Pihlstrom BL, Michalowicz BS, Johnson NW. Periodontal diseases. Lancet 2005; 366(9499):1809–20.
[5] Kinane DF, Stathopoulou PG, Papapanou PN. Periodontal diseases. Nat Rev Dis Prim 2017;3:17038.
[6] Abdulkareem AA, Al-Taweel FB, Al-Sharqi AJB, Gul SS, Sha A, Chapple ILC. Current concepts in the pathogenesis of periodontitis: from symbiosis to dysbiosis. J Oral Microbiol 2023;15(1):2197779.
[7] Hajishengallis G. Periodontitis: from microbial immune subversion to systemic inflammation. Nat Rev Immunol 2015;15(1):30–44.
[8] Sedghi LM, Bacino M, Kapila YL. Periodontal disease: the good, the bad, and the unknown. Front Cell Infect Microbiol 2021;11.
[9] Darveau RP. Periodontitis: a polymicrobial disruption of host homeostasis. Nat Rev Microbiol 2010;8(7):481–90.
[10] Könönen E, Gursoy M, Gursoy UK. Periodontitis: a multifaceted disease of tooth-supporting tissues. J Clin Med 2019;8(8):1135.
[11] Hajishengallis G, Chavakis T, Lambris JD. Current understanding of periodontal disease pathogenesis and targets for host-modulation therapy. Periodontology 2020;84(1):14–34. 2000.
[12] Hajishengallis G. Immunomicrobial pathogenesis of periodontitis: keystones, pathobionts, and host response. Trends Immunol 2014;35(1):3–11.
[13] Buduneli N. Environmental factors and periodontal microbiome. Periodontology 2021;85(1):112–25. 2000.
[14] Scannapieco FA, Dongari-Bagtzoglou A. Dysbiosis revisited: understanding the role of the oral microbiome in the pathogenesis of gingivitis and periodontitis: a critical assessment. J Periodontol 2021;92(8):1071–8.
[15] Teles F, Wang Y, Hajishengallis G, Hasturk H, Marchesan JT. Impact of systemic factors in shaping the periodontal microbiome. Periodontology 2021;85(1): 126–60. 2000.
[16] Li X, Kolltveit KM, Tronstad L, Olsen I. Systemic diseases caused by oral infection. Clin Microbiol Rev 2000;13(4):547–58.
[17] Hajishengallis G, Chavakis T. Local and systemic mechanisms linking periodontal disease and inflammatory comorbidities. Nat Rev Immunol 2021;21(7):426–40.
[18] Kapila YL. Oral health's inextricable connection to systemic health: special populations bring to bear multimodal relationships and factors connecting periodontal disease to systemic diseases and conditions. Periodontology 2021;87 (1):11–6. 2000.
[19] Hannig C, Hannig M. The oral cavity—a key system to understand substratum-dependent bioadhesion on solid surfaces in man. Clin Oral Invest 2009;13(2): 123–39.
[20] Souza JGS, Costa RC, Sampaio AA, Abdo VL, Nagay BE, Castro N, Retamal-Valdes B, Shibli JA, Feres M, Barão VAR, Bertolini M. Cross-kingdom microbial interactions in dental implant-related infections: is Candida albicans a new villain? iScience 2022;25(4):103994.
[21] Tu Y, Ren H, He Y, Ying J, Chen Y. Interaction between microorganisms and dental material surfaces: general concepts and research progress. J Oral Microbiol 2023;15(1):2196897.
[22] Song F, Koo H, Ren D. Effects of material properties on bacterial adhesion and biofilm formation. J Dent Res 2015;94(8):1027–34.
[23] Zheng S, Bawazir M, Dhall A, Kim H-E, He L, Heo J, Hwang G. Implication of surface properties, bacterial motility, and hydrodynamic conditions on bacterial surface sensing and their initial adhesion. Front Bioeng Biotechnol 2021;9(82).
[24] Schmalz G, Cieplik F. Biofilms on restorative materials. Oral Biofilms 2021;29: 155–94.
[25] Quirynen M, Brecx M, Van Steenberghe D, Evans LV. Biofilms in the oral cavity: impact of surface characteristics. In: Biofilms: recent advances in their study and control. Amsterdam: Harwood Academic Publishers; 2000. p. 167–87.
[26] Alarcón-Sánchez MA, Heboyan A, Fernandes GVO, Castro-Alarcón N, Romero-Castro NS. Potential impact of prosthetic biomaterials on the periodontium: a comprehensive review. Molecules 2023;28(3).
[27] Ababnaeh KT, Al-Omari M, Alawneh TN. The effect of dental restoration type and material on periodontal health. Oral Health Prev Dent 2011;9(4):395–403.
[28] Schmidt JC, Sahrmann P, Weiger R, Schmidlin PR, Walter C. Biologic width dimensions–a systematic review. J Clin Periodontol 2013;40(5):493–504.
[29] Paolantonio M, D'Ercole S, Perinetti G, Tripodi D, Catamo G, Serra E, Bruè C, Piccolomini R. Clinical and microbiological effects of different restorative materials on the periodontal tissues adjacent to subgingival class V restorations. J Clin Periodontol 2004;31(3):200–7.
[30] Padbury Jr A, Eber R, Wang HL. Interactions between the gingiva and the margin of restorations. J Clin Periodontol 2003;30(5):379–85.
[31] Jiang Y, Brandt BW, Buijs MJ, Cheng L, Exterkate RAM, Crielaard W, Deng DM. Manipulation of saliva-derived microcosm biofilms to resemble dysbiotic subgingival microbiota. Appl Environ Microbiol 2021;87(3).
[32] Baraniya D, Naginyte M, Chen T, Albandar JM, Chialastri SM, Devine DA, Marsh PD, Al-hebshi NN. Modeling normal and dysbiotic subgingival microbiomes: effect of nutrients. J Dent Res 2020;99(6):695–702.
[33] Cieplik F, Zaura E, Brandt BW, Buijs MJ, Buchalla W, Crielaard W, Laine ML, Deng DM, Exterkate RAM. Microcosm biofilms cultured from different oral niches in periodontitis patients. J Oral Microbiol 2019;11(1):1551596.
[34] Hakimeh S, Vaidyanathan J, Houpt ML, Vaidyanathan TK, Von Hagen S, School NJD. Microleakage of compomer class V restorations: effect of load cycling, thermal cycling, and cavity shape differences. J Prosthet Dent 2000;83 (2):194–203.

[35] Montoya C, Kurylec J, Ossa A, Orrego S. Cyclic strain of poly (methyl methacrylate) surfaces triggered the pathogenicity of Candida albicans. Acta Biomater 2023;170:415–26.
[36] Passanezi E, Sant'Ana ACP. Role of occlusion in periodontal disease. Periodontology 2019;79(1):129–50. 2000.
[37] Zhu R, Zhang Z, Lu B, Zhang P, Liu W, Liang X. Unloading of occlusal force aggravates alveolar bone loss in periodontitis. J Periodontal Res 2022;57(5): 1070–82.
[38] Schröder A, Käppler P, Nazet U, Jantsch J, Proff P, Cieplik F, Deschner J, Kirschneck C. Effects of compressive and tensile strain on macrophages during simulated orthodontic tooth movement. Mediat Inflamm 2020;2020:2814015.
[39] Varghese SS. Influence of angles occlusion in periodontal diseases. Bioinformation 2020;16(12):983–91.
[40] Deas DE, Mealey BL. Is there an association between occlusion and periodontal destruction?: only in limited circumstances does occlusal force contribute to periodontal disease progression. England J Am Dent Assoc 2006:1381. 1383, 1385 passim.
[41] Dederichs M, Joedecke P, Weber C-T, Guentsch A. Functional load capacity of teeth with reduced periodontal support: a finite element analysis. Bioengineering 2023;10(11):1330.
[42] Daghrery A, Bottino MC. Advanced biomaterials for periodontal tissue regeneration. Genesis 2022;60(8–9):e23501.
[43] Zhu Y, Tao C, Goh C, Shrestha A. Innovative biomaterials for the treatment of periodontal disease. Front. Dent. Med. 2023;4.
[44] Montoya C, Roldan L, Yu M, Valliani S, Ta C, Yang M, Orrego S. Smart dental materials for antimicrobial applications. Bioact Mater 2023;24:1–19.
[45] Jiao Y, Tay FR, Niu L-n, Chen J-h. Advancing antimicrobial strategies for managing oral biofilm infections. Int J Oral Sci 2019;11(3):1–11.
[46] Nasiri K, Masoumi SM, Amini S, Goudarzi M, Tafreshi SM, Bagheri A, Yasamineh S, alwan M, Arellano MTC, Gholizadeh O. Recent advances in metal nanoparticles to treat periodontitis. J Nanobiotechnol 2023;21(1):283.
[47] Luan J, Li R, Xu W, Sun H, Li Q, Wang D, Dong S, Ding J. Functional biomaterials for comprehensive periodontitis therapy. Acta Pharm Sin B 2023;13(6):2310–33.
[48] Montoya C, Jain A, Londoño J, Correa S, Lelkes P, Melo M, Orrego S. Multifunctional dental composite with piezoelectric nano-fillers for both antibiofilm and remineralization therapies. 2021. submitted for publication.
[49] Montoya C, Kurylec J, Baraniya D, Tripathi A, Puri S, Orrego S. Antifungal effect of piezoelectric charges on PMMA dentures. ACS Biomater Sci Eng 2021;7(10): 4838–46.
[50] Roldan L, Montoya C, Solanki V, Cai KQ, Yang M, Correa S, Orrego S. A novel injectable piezoelectric hydrogel for periodontal disease treatment. ACS Appl Mater Interfaces 2023;15(37):43441–54.
[51] Maktabi H, Ibrahim M, Alkhubaizi Q, Weir M, Xu H, Strassler H, Fugolin APP, Pfeifer CS, Melo MAS. Underperforming light curing procedures trigger detrimental irradiance-dependent biofilm response on incrementally placed dental composites. J Dent 2019;88:103110.
[52] Habibah TU, Amlani DV, Brizuela M. Hydroxyapatite dental material. 2018.
[53] Bollen CM, Lambrechts P, Quirynen M. Comparison of surface roughness of oral hard materials to the threshold surface roughness for bacterial plaque retention: a review of the literature. Dent Mater 1997;13(4):258–69.
[54] Fischer NG, Aparicio C. The salivary pellicle on dental biomaterials. Colloids Surf B Biointerfaces 2021;200:111570.
[55] Al-Ahmad A, Wollensak K, Rau S, Guevara Solarte DL, Paschke S, Lienkamp K, Staszewski O. How do polymer coatings affect the growth and bacterial population of a biofilm formed by total human salivary bacteria?-A study by 16S-rna sequencing. Microorganisms 2021;9(7).
[56] W.J. Syed Sa Fau - Loesche, W.J. Loesche, Survival of human dental plaque flora in various transport media, (0003-6919 (Print))..
[57] Sato Y, Yamagishi J, Yamashita R, Shinozaki N, Ye B, Yamada T, Yamamoto M, Nagasaki M, Tsuboi A. Inter-individual differences in the oral bacteriome are greater than intra-day fluctuations in individuals. PLoS One 2015;10(6): e0131607.
[58] Baraniya D, Do T, Chen T, Albandar JM, Chialastri SM, Devine DA, Marsh PD, Al-Hebshi NN. Optimization of conditions for in vitro modeling of subgingival normobiosis and dysbiosis. Front Microbiol 2022;13:1031029.
[59] Mestres E, García-Jiménez M, Casals A, Cohen J, Acacio M, Villamar A, Matia-Algué Q, Calderón G, Costa-Borges N. Factors of the human embryo culture system that may affect media evaporation and osmolality. Hum Reprod 2021;36 (3):605–13.
[60] Ausiello P, Ciaramella S, Martorelli M, Lanzotti A, Gloria A, Watts DC. CAD-FE modeling and analysis of class II restorations incorporating resin-composite, glass ionomer and glass ceramic materials. Dent Mater 2017;33(12):1456–65.
[61] Frank Jeremy A, Reich Claudia I, Sharma S, Weisbaum Jon S, Wilson Brenda A, Olsen Gary J. Critical evaluation of two primers commonly used for amplification of bacterial 16S rRNA genes. Appl Environ Microbiol 2008;74(8):2461–70.
[62] Lane DJ, Pace B, Olsen GJ, Stahl DA, Sogin ML, Pace NR. Rapid determination of 16S ribosomal RNA sequences for phylogenetic analyses. Proc Natl Acad Sci U S A 1985;82(20):6955–9.
[63] Zhang J, Kobert K, Flouri T, Stamatakis A. PEAR: a fast and accurate Illumina Paired-End reAd mergeR. Bioinformatics 2014;30(5):614–20.
[64] Schloss Patrick D, Westcott Sarah L, Ryabin T, Hall Justine R, Hartmann M, Hollister Emily B, Lesniewski Ryan A, Oakley Brian B, Parks Donovan H, Robinson Courtney J, Sahl Jason W, Stres B, Thallinger Gerhard G, Van Horn David J, Weber Carolyn F. Introducing mothur: open-source, platform-independent, community-supported software for describing and comparing microbial communities. Appl Environ Microbiol 2009;75(23):7537–41.
[65] Al-hebshi NN, Nasher AT, Maryoud MY, Homeida HE, Chen T, Idris AM, Johnson NW. Inflammatory bacteriome featuring Fusobacterium nucleatum and Pseudomonas aeruginosa identified in association with oral squamous cell carcinoma. Sci Rep 2017;7(1):1–10.
[66] Al-Hebshi NN, Nasher AT, Idris AM, Chen T. Robust species taxonomy assignment algorithm for 16S rRNA NGS reads: application to oral carcinoma samples. J Oral Microbiol 2015;7:28934.
[67] Caporaso JG, Kuczynski J, Stombaugh J, Bittinger K, Bushman FD, Costello EK, Fierer N, Pena AG, Goodrich JK, Gordon JI. QIIME allows analysis of high-throughput community sequencing data. Nat Methods 2010;7(5):335.
[68] Xia Y, Sun J, Chen D-G. Statistical analysis of microbiome data with R. Springer; 2018.
[69] McMurdie PJ, Holmes S. Phyloseq: an R package for reproducible interactive analysis and graphics of microbiome census data. PLoS One 2013;8(4):e61217.
[70] Mallick H, Rahnavard A, McIver LJ, Ma S, Zhang Y, Nguyen LH, Tickle TL, Weingart G, Ren B, Schwager EH, Chatterjee S, Thompson KN, Wilkinson JE, Subramanian A, Lu Y, Waldron L, Paulson JN, Franzosa EA, Bravo HC, Huttenhower C. Multivariable association discovery in population-scale meta-omics studies. PLoS Comput Biol 2021;17(11):e1009442.
[71] Chen T, Marsh PD, Al-Hebshi NN. SMDI: an index for measuring subgingival microbial dysbiosis. J Dent Res 2022;101(3):331–8.
[72] Howard KC, Gonzalez OA, Garneau-Tsodikova S. Porphyromonas gingivalis: where do we stand in our battle against this oral pathogen? RSC Med Chem 2021; 12(5):666–704.
[73] Martínez-García M, Hernández-Lemus E. Periodontal inflammation and systemic diseases: an overview. Front Physiol 2021;12:709438.
[74] Sudhakara P, Gupta A, Bhardwaj A, Wilson A. Oral dysbiotic communities and their implications in systemic diseases. Dent J 2018;6(2).
[75] Nazir MA. Prevalence of periodontal disease, its association with systemic diseases and prevention. Int J Health Sci 2017;11(2):72–80.
[76] Kilian M, Chapple ILC, Hannig M, Marsh PD, Meuric V, Pedersen AML, Tonetti MS, Wade WG, Zaura E. The oral microbiome – an update for oral healthcare professionals. Br Dent J 2016;221(10):657–66.
[77] Ausenda F, Rasperini G, Acunzo R, Gorbunkova A, Pagni G. New perspectives in the use of biomaterials for periodontal regeneration. Materials 2019;12(13).
[78] Luo TL, Vanek ME, Gonzalez-Cabezas C, Marrs CF, Foxman B, Rickard AH. In vitro model systems for exploring oral biofilms: from single-species populations to complex multi-species communities. J Appl Microbiol 2022;132(2):855–71.
[79] Chen L, McCrate JM, Lee JC, Li H. The role of surface charge on the uptake and biocompatibility of hydroxyapatite nanoparticles with osteoblast cells. Nanotechnology 2011;22(10):105708.
[80] Botelho CM, Lopes MA, Gibson IR, Best SM, Santos JD. Structural analysis of Si-substituted hydroxyapatite: zeta potential and X-ray photoelectron spectroscopy. J Mater Sci Mater Med 2002;13(12):1123–7.
[81] Hiltunen AK, Savijoki K, Nyman TA, Miettinen I, Ihalainen P, Peltonen J, Fallarero A. Structural and functional dynamics of Staphylococcus aureus biofilms and biofilm matrix proteins on different clinical materials. Microorganisms 2019;7(12).
[82] McKittrick J, Chen PY, Tombolato L, Novitskaya EE, Trim MW, Hirata GA, Olevsky EA, Horstemeyer MF, Meyers MA. Energy absorbent natural materials and bioinspired design strategies: a review. Mater Sci Eng C 2010;30(3):331–42.
[83] M. Salerno, S. Derchi G Fau - Thorat, L. Thorat S Fau - Ceseracciu, R. Ceseracciu L Fau - Ruffilli, A.C. Ruffilli R Fau - Barone, A.C. Barone, Surface morphology and mechanical properties of new-generation flowable resin composites for dental restoration, (1879-0097 (Electronic)).[.
[84] Choi S, Jo Y-H, Luke Yeo I-S, Yoon H-I, Lee J-H, Han J-S. The effect of surface material, roughness and wettability on the adhesion and proliferation of Streptococcus gordonii, Fusobacterium nucleatum and Porphyromonas gingivalis. J Dent Sci 2023;18(2):517–25.
[85] Park SH, Kim K, Cho S, Chung DH, Ahn SJ. Variation in adhesion of Streptococcus mutans and Porphyromonas gingivalis in saliva-derived biofilms on raw materials of orthodontic brackets. Korean J Orthod 2022;52(4):278–86.
[86] Cugini C, Shanmugam M, Landge N, Ramasubbu N. The role of exopolysaccharides in oral biofilms. J Dent Res 2019;98(7):739–45.
[87] Jakubovics NS, Goodman SD, Mashburn-Warren L, Stafford GP, Cieplik F. The dental plaque biofilm matrix. Periodontol 2021;86(1):32–56. 2000.
[88] Flemming HC, Wingender J. The biofilm matrix. Nat Rev Microbiol 2010;8(9): 623–33.
[89] Karygianni L, Ren Z, Koo H, Thurnheer T. Biofilm matrixome: extracellular components in structured microbial communities. Trends Microbiol 2020;28(8): 668–81.
[90] King MM, Kayastha BB, Franklin MJ, Patrauchan MA. Calcium regulation of bacterial virulence. Adv Exp Med Biol 2020;1131:827–55.
[91] Wang T, Flint S, Palmer J. Magnesium and calcium ions: roles in bacterial cell attachment and biofilm structure maturation. Biofouling 2019;35(9):959–74.
[92] Shokeen B, Pham E, Esfandi J, Kondo T, Okawa H, Nishimura I, Lux R. Effect of calcium ion supplementation on oral microbial composition and biofilm formation in vitro. Microorganisms 2022;10(9).
[93] Das T, Sehar S, Koop L, Wong YK, Ahmed S, Siddiqui KS, Manefield M. Influence of calcium in extracellular DNA mediated bacterial aggregation and biofilm formation. PLoS One 2014;9(3):e91935.
[94] Quan K, Hou J, Zhang Z, Ren Y, Peterson BW, Flemming HC, Mayer C, Busscher HJ, van der Mei HC. Water in bacterial biofilms: pores and channels, storage and transport functions. Crit Rev Microbiol 2022;48(3):283–302.

[95] Melaugh G, Hutchison J, Kragh KN, Irie Y, Roberts A, Bjarnsholt T, Diggle SP, Gordon VD, Allen RJ. Shaping the growth behaviour of biofilms initiated from bacterial aggregates. PLoS One 2016;11(3):e0149683.
[96] Yang L, Yang Y, Wang S, Li Y, Zhao Z. In vitro mechanical loading models for periodontal ligament cells: from two-dimensional to three-dimensional models. Arch Oral Biol 2015;60(3):416–24.
[97] Hasani Z, Khodadadi E, Ezoji F, Khafri S. Effect of mechanical load cycling on microleakage of restorative glass ionomers compared to flowable composite resin in class V cavities. Front Dent 2019;16(2):136–43.
[98] Ameri H, Ghavamnasiri M, Abdoli E. Effects of load cycling on the microleakage of beveled and nonbeveled margins in class V resin-based composite restorations. J Contemp Dent Pract 2010;11(5):25–32.
[99] Song WS, Lee JK, Park SH, Um HS, Lee SY, Chang BS. Comparison of periodontitis-associated oral biofilm formation under dynamic and static conditions. J Periodontal Implant Sci 2017;47(4):219–30.
[100] Picioreanu C, Van Loosdrecht MC, Heijnen JJ. Effect of diffusive and convective substrate transport on biofilm structure formation: a two-dimensional modeling study. Biotechnol Bioeng 2000;69(5):504–15.
[101] Fernández CE, Aspiras MB, Dodds MW, González-Cabezas C, Rickard AH. The effect of inoculum source and fluid shear force on the development of in vitro oral multispecies biofilms. J Appl Microbiol 2017;122(3):796–808.
[102] Paramonova E, Kalmykowa OJ, van der Mei HC, Busscher HJ, Sharma PK. Impact of hydrodynamics on oral biofilm strength. J Dent Res 2009;88(10):922–6.
[103] Harper CE, Hernandez CJ. Cell biomechanics and mechanobiology in bacteria: challenges and opportunities. APL Bioeng 2020;4(2):021501.
[104] Sharma Prashant K, Gibcus Marjon J, van der Mei Henny C, Busscher Henk J. Influence of fluid shear and microbubbles on bacterial detachment from a surface. Appl Environ Microbiol 2005;71(7):3668–73.
[105] Christersson CE, Glantz PO, Baier RE. Role of temperature and shear forces on microbial detachment. Scand J Dent Res 1988;96(2):91–8.
[106] Bostanci N, Belibasakis GN. Porphyromonas gingivalis: an invasive and evasive opportunistic oral pathogen. FEMS (Fed Eur Microbiol Soc) Microbiol Lett 2012; 333(1):1–9.
[107] Park J, Shokeen B, Haake SK, Lux R. Characterization of Fusobacterium nucleatum ATCC 23726 adhesins involved in strain-specific attachment to Porphyromonas gingivalis. Int J Oral Sci 2016:138–44. Copyright © 2016 The Author(s).
[108] Chen WA, Dou Y, Fletcher HM, Boskovic DS. Local and systemic effects of Porphyromonas gingivalis infection. Microorganisms 2023;11(2).
[109] Karched M, Bhardwaj RG, Asikainen SE. Coaggregation and biofilm growth of Granulicatella spp. with Fusobacterium nucleatum and Aggregatibacter actinomycetemcomitans. BMC Microbiol 2015;15(1):114.
[110] Frenkel A, Hirsch W. Spontaneous development of L forms of streptococci requiring secretions of other bacteria or sulphydryl compounds for normal growth. Nature 1961;191:728–30.
[111] Del Pozo JL, Rouse MS, Patel R. Bioelectric effect and bacterial biofilms. A systematic review. Int J Artif Organs 2008;31(9):786–95.
[112] Cao H-B, Li X-G, Wu J-C, Yu K-T, Zhang Y. Simulation of the effects of direct electric current on multispecies biofilms. Process Biochem 2003;38(8):1139–45.
[113] Hetrodt F, Lausch J, Meyer-Lueckel H, Conrads G, Apel C. Evaluation of restorative materials containing preventive additives in a secondary caries model in vitro. Caries Res 2019;53(4):447–56.
[114] Conrads G, Wendt LK, Hetrodt F, Deng ZL, Pieper D, Abdelbary MMH, Barg A, Wagner-Döbler I, Apel C. Deep sequencing of biofilm microbiomes on dental composite materials. J Oral Microbiol 2019;11(1):1617013.
[115] Ciofu O, Moser C, Jensen PØ, Høiby N. Tolerance and resistance of microbial biofilms. Nat Rev Microbiol 2022;20(10):621–35.
[116] Miranda LFB, Lima CV, Pagin R, Costa RC, Pereira MMA, de Avila ED, Bertolini M, Retamal-Valdes B, Shibli JA, Feres M, Barão VAR, Souza JGS. Effect of processing methods of human saliva on the proteomic profile and protein-mediated biological processes. J Proteome Res 2023;22(3):857–70.
[117] Balhaddad AA, Garcia IM, Mokeem L, Ibrahim MS, Collares FM, Weir MD, Xu HHK, Melo MAS. Bifunctional composites for biofilms modulation on cervical restorations. J Dent Res 2021;100(10):1063–71.
[118] Ibrahim MS, Garcia IM, Vila T, Balhaddad AA, Collares FM, Weir MD, Melo MAS. Multifunctional antibacterial dental sealants suppress biofilms derived from children at high risk of caries. Biomater Sci 2020;8(12):3472–84.
[119] Saavedra FA-O, Pelepenko LA-O, Boyle WS, Zhang A, Staley CA-O, Herzberg MC, Marciano MA, Lima BA-O. In vitro physicochemical characterization of five root canal sealers and their influence on an ex vivo oral multi-species biofilm community. Int Endod J 2022;55:1365–2591 (Electronic).
[120] Onyango Stanley O, De Clercq N, Beerens K, Van Camp J, Desmet T, Van de Wiele T. Oral microbiota display profound differential metabolic kinetics and community shifts upon incubation with sucrose, trehalose, kojibiose, and xylitol. Appl Environ Microbiol 2020;86(16):e01170. 20.
[121] Poeker SA, Lacroix C, de Wouters T, Spalinger MR, Scharl M, Geirnaert A. Stepwise development of an in vitro continuous fermentation model for the murine caecal microbiota. Front Microbiol 2019;10.
[122] Shi M, Wei Y, Hu W, Nie Y, Wu X, Lu R. The subgingival microbiome of periodontal pockets with different probing depths in chronic and aggressive periodontitis: a pilot study. Front Cell Infect Microbiol 2018;8:124.